Proc. of the International Conference on Mechanical, Automotive and Mechatronics Engineering (ICMAME 2023)
29-30 April 2023, Dubai, UAE

Bearing Fault Detection Scheme Using Machine Learning for Condition Monitoring Applications

Ali Saad
Dept. of Mechanical Engineering,
COMSATS University Islamabad,
Wah Campus, Wah Cantt., Pakistan
engr.alisaad@gmail.com

Ali Usman
EISLAB, Machine Learning,
Luleå University of Technology,
Luleå, Sweden
ali.usman@ltu.se

Saad Arif
Dept. of Mechanical Engineering,
HITEC University Taxila,
Taxila Cantt., Pakistan
saad.arif@hitecuni.edu.pk

Marcus Liwicki
Department of Computer Science,
Luleå University of Technology,
Luleå, Sweden
marcus.liwicki@ltu.se

Andreas Almqvist
Division of Machine Elements,
Luleå University of Technology,
Luleå, Sweden
Andreas.Almqvist@ltu.se

***Abstract*—Bearings are the significant components among the rolling machine elements subjected to high wear and tear. The timely detection of faults in such components rotating at higher frequencies can save substantial maintenance costs and production setbacks. Physical examination and fault detection by human experts is always challenging at runtime. Predictive maintenance and real-time condition monitoring are gaining higher utility with the advent of suitable instrumentation and machine learning classifiers. A convolutional neural network (CNN) based bearing fault detection scheme is developed in this research work. The acquired sensory data of vibration signals are converted into the frequency domain and then fed to the classifier for spectral feature extraction and fault classification. The CNN architecture is trained and tested using a bearing dataset available online. The model is further tested and validated with the data acquired from an indigenously designed bearing test rig. The proposed scheme has successfully detected inner and outer race faults and no fault or normal state. This multiclass fault classification has shown promising results with 97.68% accuracy, 96.9% precision, 99.14% sensitivity, 98.01% F_1-score, and 93.65% specificity. The achieved results validate the utility of the proposed detection system. Hence the presented scheme has deployment potential for real-time condition monitoring and predictive maintenance applications.**

Keywords—vibrations, rolling elements, machine learning, fault detection, condition monitoring, predictive maintenance

I. Introduction

A substantial shift is observed in the adapted approach of the current maintenance industry. A significant inclination towards condition-based or predictive maintenance methods is in practice nowadays. The pattern analysis of various parameters involved in the machinery failure modes significantly avoids cost and production setbacks. A successful machine condition monitoring technique is thought to be capable of detecting the root cause of the defect, its accurate diagnosis, and the location of its possible resurfacing. However, specialized instruments and advanced technological devices for machine health assessment are effective solutions meantime incurring heavy cost overheads. However, one is looking for creative solutions for the challenges faced in monitoring complex, expensive, and fragile industrial machine applications. Artificial intelligence (AI) has recently made substantial technological strides in intelligent diagnosis with cost-effective data-driven approaches. AI-based intelligent methods are superior to conventional methods for machine fault diagnosis. Rolling elements fault detection is a technique that helps to detect defects in rotary elements of machines. The technique uses neural networks to identify the faults in the rolling elements. The neural networks are well-trained with the sensory data acquired from the machines and can be used to predict when a rolling element fault will occur effectively. The neural networks can learn the numerical and image data features to classify various applications. Its multilayered architecture can learn the output classes with weighted interconnections between input, hidden, and output layers. This non-linear modeling technique can efficiently learn the highly complex models for which analytical relationships are hard to develop and even less performing.

In this research work, a convolutional neural network (CNN)-based fault classification model is designed, tested, and validated for rolling machine element condition monitoring applications. The rest of the manuscript includes: a detailed literature review in section II, the design methodology explained in section III, results discussed in section IV, and finally, the study is concluded in section V.

II. Literature Review

A diagnostic system keeps track of a limited number of adequately categorized failure modes chosen after investigating their acute effects, causes, and failure types. These defects can lead to faulty installation, inadequate track alignment, or unbalanced loading of subsequent components [1, 2]. These defects could appear as wear when the rolling elements' raceways develop a recess, cracking, and abrasives because of overloading and inadequate lubrication. The corrosion caused by the pitting of the raceways and the bearing surface, together with the inclusion of moisture between the load bearing sections, causes crack propagation [3, 4]. One of the most common causes of rolling bearing failure is chipping from the raceways or rolling elements. It starts as a fatigue crack that extends beneath the metal surface and propagates along the race until a fragment of metal shatters and leaves a little pit or chip. Physics-based models for tracking the bearing status are also developed [5, 6].

In predictive maintenance applications, the artificial neural network (ANN) is implemented on low-cost microcontrollers for non-invasive intelligent condition monitoring of induction motors. Kalman filter is used for vibration data denoising. The ANN, along with vibration and thermal analysis, provides efficient and accurate remote condition monitoring access without the physical intervention of humans [7]. The data-driven AI approaches

are effectively being developed to access tool wear and bearing failure modes. These research directions investigate the intensive use of predictive maintenance approaches toward Industry 4.0 applications [8-10]. The ANN is gaining popularity in machine status monitoring and problem diagnosis involving acoustic emission signal analysis and AI techniques. Condition monitoring in compliance with fault detection and diagnosis systems becomes imperative for better detection, diagnosis, monitoring, and prognosis. Acoustic emission has been used to extract the acoustic signal from a gas pipeline having valve leakage. The measured acoustic emission characteristic is then used in the time and frequency domains interpreted as leakage features [11]. The AI-based machine learning algorithm, the support vector machines, and the genetic algorithm (GA) proved to achieve better results in such condition-monitoring applications where GA is used for feature selection in this study [11].

III. Design Methodology

A SqueezeNet-based CNN architecture is used in this study to perform bearing faults classification [12-14]. The pre-trained network is retrained using transfer learning to classify bearing scalogram images. This network training is performed over the online available bearing fault dataset with 10-fold cross-validation. The trained network is then tested and validated to classify the scalograms obtained for the data acquired from an indigenously designed bearing test rig. During real-time experimentation, the fault diagnosing module generates fault feedback in the form of an audio warning signal and a visual optical flag in the control room of the condition monitoring and maintenance center. Fig. 1 shows the block diagram and process flow of the complete methodology adapted for the fault classification scheme.

A. NICE Bearing Data Set

A dataset on bearing faults has been made available by the Machinery Failure Prevention Technology (MFPT) society to aid in the study of bearing analysis. This fault dataset consists of two types of NICE bearing faults obtained from the MFPT database, which have flaws of the outer race face, inner race face, and the standard ball bearing data [15, 16].

The data set obtained from the mentioned source comprises three sets of baseline conditions with no fault (NF), seven outer race fault (ORF), and seven inner race fault (IRF) conditions. The complete dataset is imported in MATLAB 9.12 (MathWorks, USA) with its .mat file and is further used to retrain CNN and apply different algorithms. The dataset is comprised of bearing load, operating frequency, data sampling rate, and 3-dimensional acceleration vector with g-values along with the fault mentioned above labels.

B. SKF 6202 Bearing Test Rig

The SKF 6202 ball bearing-based test rig is designed to conduct repeated experiments. The multiple test sessions were conducted to acquire time series vibrational data with faulty and standard bearings mounted at the test rig. The accelerometer data is acquired in the computer via serial interface and recorded in CSV file format for 50 seconds epoch during each experiment. The operating speed of the shaft is set to 3000 revolutions per minute (RPM) during the data recording event. The labeled experimental data is recorded for all three defined classes (IRF, ORF, and NF) for each session. The following design parameters of the SKF 6202 bearing have been incorporated in the mathematical modeling before the train and test data preparation. The cross-sectional view of the bearing and involved parameters are indicated in Fig. 2.

The ball pass outer race frequency (BPFO) is the number of occurrences for which a rolling element or ball bearing traverses a specific location at the outer race of the bearing. It is determined with the equation below.

$$BPFO = \frac{nf_r}{2}\left(1 - \frac{d}{D}\cos\emptyset\right) \quad (1)$$

The ball pass inner race frequency (BPFI) is determined using the following relationship. BPFI refers to the number of times a rolling element or ball bearing passes at a specific position at the inner race of the bearing.

$$BPFI = \frac{nf_r}{2}\left(1 + \frac{d}{D}\cos\emptyset\right) \quad (2)$$

where n is the number of rolling elements, f_r is the shaft speed, d is the diameter of the ball bearing, D is the pitch diameter, and $\emptyset$ is the bearing angle of contact with the races. $\emptyset$ is determined using the Turns method or with the measurement of internal clearance. It is set as 25° by the manufacturer for SKF 6202 bearing.

C. Data Preparation and Model Training

The recorded dataset is then prepared for transfer learning of the SqueezeNet CNN model. The time series vibration signal for the entire experimental epoch is converted into the time-frequency domain with 1D continuous wavelet transform (CWT). This converted data is used to generate CWT scalograms as shown in Fig. 3. The CWT scalogram images are created using the *cwt* built-in function of MATLAB 9.12. These images hold bearing state information

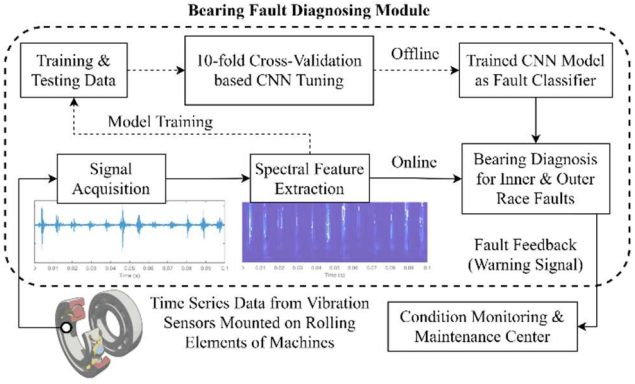

Fig. 1. Block diagram and process flow of bearing fault detection system

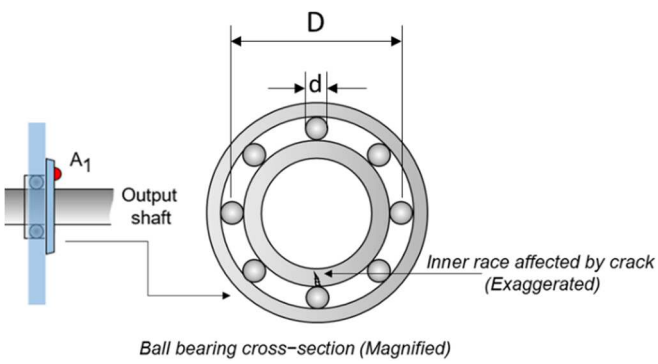

Fig. 2. SKF 6202 ball bearing cross-section showing design parameters

in terms of CWT magnitude at particular frequencies, synchronously with occurrence time information.

After training dataset preparation, the SqueezeNet CNN architecture is created in MATLAB 9.12 with its *squeezenet* built-in function. The required changes in the CNN model are performed to classify the labeled scalogram images. For model transfer learning, the last learnable layer and final layer are replaced with a new 2D convolutional layer and a new classification layer to retrain the SqueezeNet with scalogram image data and to adapt to the new target classes. The new convolutional layer has three filters of 1×1 size as per three output classes. The weight and bias learning rate factors are set to 10. The model used stochastic gradient descent with momentum (sgdm) optimizer for convergence. The final CNN architecture has a total 68 number of layers from the input to the output layer. After incorporating the required architectural changes, the cross-validated training process is initiated. The CNN model takes the labeled CWT scalogram images of size 227×227×3 as the input and returns the predicted class label of bearing condition together with the probabilities against each class. The model is fine-tuned by testing over 80% of the total images from the database. The practical and rich feature extraction from input images with decreasing the number of CNN parameters and increasing accuracy are some of the benefits of this efficient CNN algorithm.

D. Experimental Data Classification

The exact initial procedure of dataset preparation is applied to the experimental data obtained from the SKF 6202 test rig. The CWT scalograms are created from the acquired time series data and fed to the trained CNN model for fault classification. The state identification on testing data is made in different experiments comprising small batch sizes of almost the same epoch lengths used for the model training. The fault classification performance is evaluated with the help of confusion matrix-based assessment metrics.

E. Classification Performance Assessment

The confusion matrix and related metrics are efficient tools for analyzing the performance results of binary and multiclass classification tasks in machine learning applications [17, 18]. Following confusion matrix-based assessment metrics are used to represent the classification results.

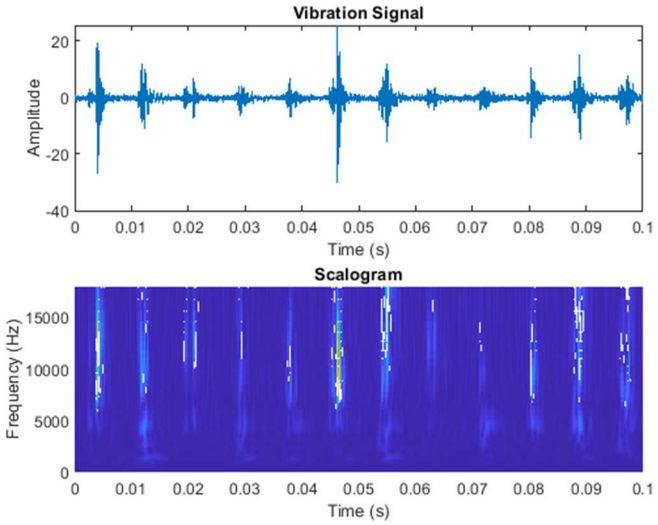

Fig. 3. Time series plot (top) and CWT scalogram (bottom) for vibration data

$$Accuracy = \frac{TP+TN}{TP+FN+FP+TN} \times 100\% \quad (3)$$

$$Precision, PPV = \frac{TP}{TP+FP} \times 100\% \quad (4)$$

$$Recall, Sensitivity, TPR = \frac{TP}{TP+FN} \times 100\% \quad (5)$$

$$F_1\ score = \frac{2\times TP}{2\times TP+FP+FN} \times 100\% \quad (6)$$

$$Specificity, TNR = \frac{TN}{FP+TN} \times 100\% \quad (7)$$

where TP, TN, FP, FN, PPV, TPR, and TNR are the true positive, true negative, false positive, false negative, positive predictive value, true positive rate, and true negative rate, respectively. The other three important metrics are the miss rate, fall-out, and false discovery rate (FDR), which are the converse terms of TPR, TNR, and PPV, respectively. In addition, the receiver operating characteristics (ROC) curve and the area under the curve (AUC) are also used to ascertain the promising performance of the classifier. All these metrics are obtained in MATLAB 9.12 with the *confusionchart* and the *perfcurve* functions. The class imbalance due to the varying number of observations in each class is also accounted for during the performance analysis [19, 20].

F. Bearing Fault Detection Scheme

An adaptive bearing fault detection scheme is developed which effectively adjusts the detection criteria for any new or replaced bearing. The state classification result of the CNN model in terms of occurrence rates of each class (ORF, IRF, NF) in a fixed adaptation period t_{adapt} are recorded for each healthy bearing. These occurrence rates are set as threshold or reference values for the normal or healthy operation of that bearing. A fault detection controller continuously measures the class occurrence rates and compares them against the threshold rates in a 5-second cycle. At the end of each cycle, if either ORF or IRF rate deviates with +2σ, and the NF rate deviates by -2σ from the threshold value as zero mean, the controller generates the warning signal as fault feedback for the control center.

IV. Results and Discussion

The CWT scalogram images hold promising state features embedded into them in terms of absolute continuous wavelet transform bounded with the occurrence time information [21]. The high amplitude spikes in the vibration signal in a particular frequency band can be assessed from the scalogram. The higher CWT magnitude is represented with white spikes in the scalogram image for the entire experimental epoch, as shown in Fig. 3. These increased CWT spikes represent the bearing fault occurrences in terms of features. While the normal condition does not show a significantly higher magnitude of CWT which is represented in blue color. The CNN model performs feature extraction from these images without losing critical information required to classify the bearing state [22]. It efficiently detects the IRF, ORF, and NF bearing states.

Fig. 4 shows the SqueezeNet CNN retraining performance history over the NICE-bearing dataset. The learning process is converged in four training cycles with 41 iterations per epoch and 164 iterations. The training process is completed with 10-fold cross-validation in each training cycle. Higher training loss and lower validation accuracy in 1st iteration are

subsequently improved with minimum training loss and 96.19% cumulative validation frequency at the end of 4th iteration. The transfer learning of this CNN model is effectively accomplished in significantly less training time with promising accuracy attainment.

The confusion matrices and related metrics are evaluated for all the experiments of both bearing datasets. Fig. 5 and Fig. 6 represent the confusion matrices with 97.68% and 91.82% best classification accuracies achieved for NICE and SKF 6202 bearing datasets, respectively. The diagonal and off-diagonal entries represent the correctly classified and misclassified samples against each bearing state class. Columns at the right of matrices show the normalized values of recall and miss rate (false negative rate, FNR), while the rows at the bottom of the matrices represent the normalized values of precision and FDR for each class. For NICE bearing, 346 samples of either bearing fault (IRF and ORF) and 118 samples of normal state (NF) are correctly classified out of 475 total input samples, with only 11 misclassified samples. While for SKF 6202 bearing, 323 samples of either bearing fault and 115 samples of NF state are correctly classified out of 477 total samples with 39 misclassifications. These observations represent the bearing state detection capability of the proposed CNN classifier, as shown by the achieved validation accuracies.

The overall efficiency of the CNN classifier for bearing fault detection can be accessed from the ROC curve [23] as shown in Fig. 7. The AUC of 0.9658 shows that the model is well-trained to classify the bearing defects effectively. This

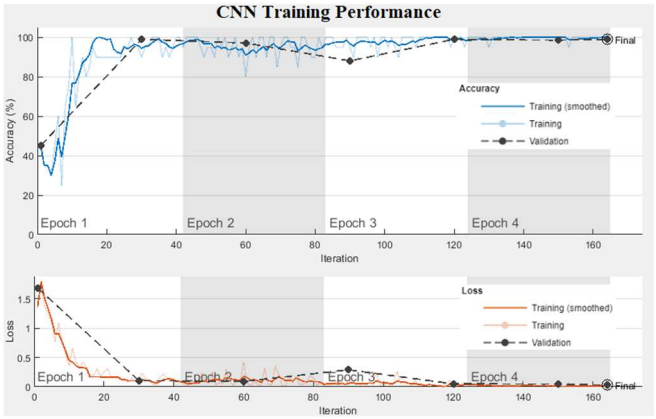

Fig. 4. CNN training history against iterations with convergence information

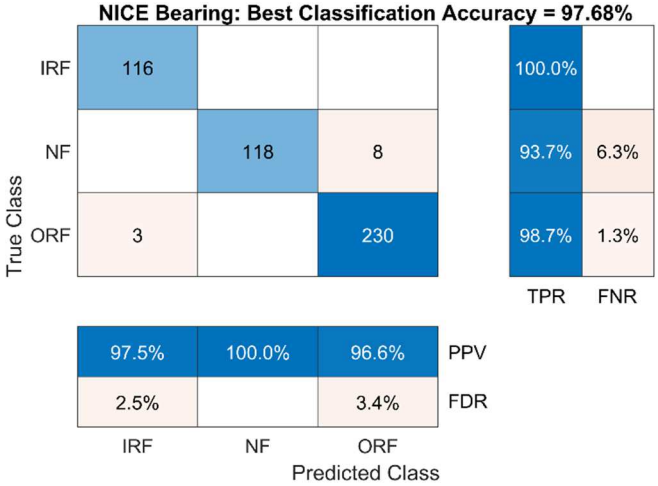

Fig. 5. Confusion matrix for NICE bearing dataset (Experiment 2)

ROC is developed for either bearing defects as a positive class aggregated with a weighted averaging technique. It shows a higher probability of fault detection when it occurs with 93.55% mean sensitivity or hit rate. Moreover, there is less probability of false detection of the bearing defect during normal bearing states with a 9.20% mean fall-out.

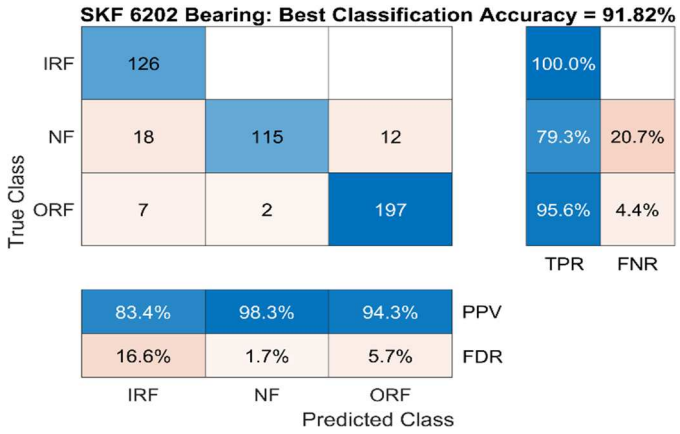

Fig. 6. Confusion matrix for SKF 6202 bearing dataset (Experiment 6)

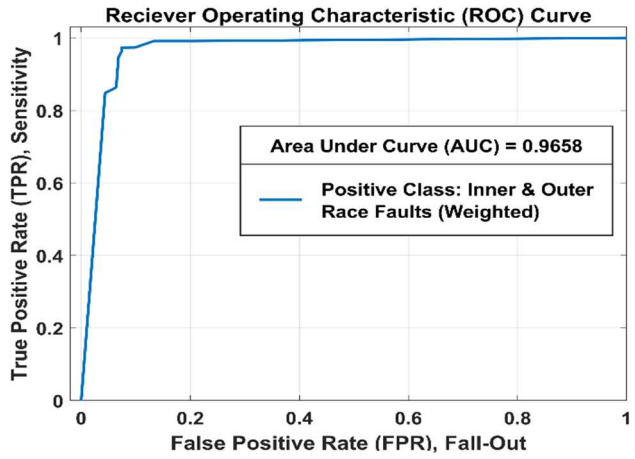

Fig. 7. ROC curve and AUC for the trained bearing fault classification model

All the performance assessment metrics are calculated for all the experimental sessions performed for both the bearing datasets, as shown in Table I. Experiment numbers 1 to 5 show the results for the NICE bearing dataset, and experiment numbers 6 to 9 show the results for SKF 6202 bearing dataset. The validation accuracy ranges from 93.40% to 97.68% for the MFPT database, while it ranges from 85.28% to 91.82% for the experimental dataset of the test rig. The reason for this difference in accuracy is that 80% of the MFPT database has been employed for CNN training. Other factors of comparatively less accuracy with the test rig dataset may include: the difference in ball bearing type and related parameters, limitations of the data acquisition system, and data imbalance, etc. Overall, the results are auspicious throughout the nine experiments. The higher accuracy, precision, recall, and F-measure indicate effective bearing fault detection and good NF state detection with higher selectivity values.

TABLE I. CONFUSION MATRICES BASED RESULTS WITH 10-FOLD CROSS-VALIDATION

Exp. no.	Performance Assessment Metrics (%)							
	Accuracy	Precision	Recall	F_1-Score	Specificity	Miss rate	Fall-out	FDR
1	97.7	96.9	99.1	98.0	93.6	0.9	6.5	3.2
2	97.7	96.9	99.1	98.0	93.6	0.9	6.4	3.2
3	96.1	94.8	96.2	95.5	95.6	3.8	4.4	5.2
4	96.3	95.7	97.4	96.5	93.2	2.6	6.8	4.3
5	93.4	92.9	94.7	93.8	90.1	5.3	9.9	7.1
6	91.8	90.1	97.3	93.5	79.3	2.7	20.7	10.0
7	87.8	85.2	86.3	85.8	92.6	13.7	7.4	14.8
8	88.4	85.7	87.0	86.3	92.6	13.0	7.4	14.3
9	85.3	83.7	84.8	84.3	86.7	15.2	13.3	16.3
Mean	92.7	91.3	93.6	92.4	90.8	6.4	9.2	8.7

On the other hand, the lower values of miss-rate, fall-out, and FDR represent fewer chances of bearing fault misclassification. All the metrics for bearing faults, i.e., IRF and ORF, are cumulatively calculated with the weighted average method to incorporate the impact of class imbalance.

V. CONCLUSIONS

This study examines the non-invasive fault classification technique for ball bearings as rolling elements. The mechanical foundation of rotary machinery is the bearing. Failure of these parts can halt operations and cause financial losses that are significantly greater than the cost of the part itself.

A data-driven condition prediction model is developed for ball bearing failure detection. The proposed classification model is comprised of a SqueezeNet-based convolutional neural network (CNN) which is retrained with transfer learning for publicly available bearing fault datasets. The other significant contribution of this study is the validation of the proposed prediction approach over the experimental data.

The cross-validated results of CNN for NICE bearing training data and SKF bearing (test rig) experimental data show promising inner and outer race bearing faults and no bearing fault condition detection. The mean values of performance assessment metrics like accuracy, precision, recall, F_1-score, specificity, miss-rate, fall-out, and false detection rate ascertain the utility of the classifier to correctly identify the bearing faults when they occur as well as rejecting them in healthy operating conditions with higher probability.

Hence, it can be concluded from the experimental results that the designed CNN architecture can be used to detect defects for various types of bearings other than that which is employed to train the network. Besides the variations in detection accuracy, the model works with reliable results for different part types and operating conditions. This factor ascertains the utility of the proposed scheme for effective condition monitoring and health prediction of rolling elements. Increasing the detection accuracy for more bearing types, classification of more bearing faults, and real-time deployment of the fault diagnostic system are the future directions of this study.

ACKNOWLEDGMENT

The Swedish Kempe Foundation has funded parts of this work. The authors would also like to acknowledge the support from the Swedish Research Council: DNR 2019-04293.

REFERENCES

[1] R. B. Randall and J. Antoni, "Rolling element bearing diagnostics—A tutorial," Mechanical systems and signal processing, vol. 25, no. 2, pp. 485–520, 2011.

[2] W. A. Smith and R. B. Randall, "Rolling element bearing diagnostics using the Case Western Reserve University data: A benchmark study," Mechanical systems and signal processing, vol. 64, pp. 100–131, 2015.

[3] T. A. Harris and M. N. Kotzalas, Advanced concepts of bearing technology: rolling bearing analysis. CRC press, 2006.

[4] K. Ranasinghe, K. Guan, A. Gardi, and R. Sabatini, "Review of advanced low-emission technologies for sustainable aviation," Energy, vol. 188, p. 115945, 2019.

[5] A. Cubillo, S. Perinpanayagam, and M. Esperon-Miguez, "A review of physics-based models in prognostics: Application to gears and bearings of rotating machinery," Advances in Mechanical Engineering, vol. 8, no. 8, p. 1687814016664660, 2016.

[6] P. Aivaliotis, Z. Arkouli, K. Georgoulias, and S. Makris, "Degradation curves integration in physics-based models: Towards the predictive maintenance of industrial robots," Robotics and computer-integrated manufacturing, vol. 71, p. 102177, 2021.

[7] M. Gana, H. Achour, K. Belaid, Z. Chelli, M. Laghrouche, and A. Chaouchi, "Non-invasive intelligent monitoring system for fault detection in induction motor based on lead-free-piezoelectric sensor using ANN," Measurement Science and Technology, vol. 33, no. 6, p. 065105, 2022.

[8] W. J. Lee, H. Wu, H. Yun, H. Kim, M. B. Jun, and J. W. Sutherland, "Predictive maintenance of machine tool systems using artificial intelligence techniques applied to machine condition data," Procedia Cirp, vol. 80, pp. 506–511, 2019.

[9] T. P. Carvalho, F. A. Soares, R. Vita, R. d. P. Francisco, J. P. Basto, and S. G. Alcalá, "A systematic literature review of machine learning methods applied to predictive maintenance," Computers & Industrial Engineering, vol. 137, p. 106024, 2019.

[10] J. Dalzochio et al., "Machine learning and reasoning for predictive maintenance in Industry 4.0: Current status and challenges," Computers in Industry, vol. 123, p. 103298, 2020.

[11] B. Ahn, J. Kim, and B. Choi, "Artificial intelligence-based machine learning considering flow and temperature of the pipeline for leak early detection using acoustic emission," Engineering Fracture Mechanics, vol. 210, pp. 381–392, 2019.

[12] N. Mohanta, R. K. Singh, J. K. Katiyar, and A. K. Sharma, "A Novel Fluid–Structure Interaction (FSI) Modeling Approach to Predict the Temperature Distribution in Single-Point Cutting Tool for Condition Monitoring During Turning Process," Arabian Journal for Science and Engineering, vol. 47, no. 7, pp. 7995–8007, 2022.

[13] L. Su, L. Ma, N. Qin, D. Huang, and A. H. Kemp, "Fault diagnosis of high-speed train bogie by residual-squeeze net," IEEE Transactions on Industrial Informatics, vol. 15, no. 7, pp. 3856–3863, 2019.

[14] N. Ceylan, S. Kaçar, E. Güney, and C. Bayilmiş, "Detection of Grinding Burn Fault in Bearings by Squeeze Net," in 30th Signal Processing and Communications Applications Conference (SIU), 2022, pp. 1–4: IEEE.

[15] M. Mohiuddin and M. S. Islam, "Rolling Element Bearing Faults Detection and Classification Technique Using Vibration Signals," Engineering Proceedings, vol. 27, no. 1, p. 53, 2022.

[16] D. Verstraete, A. Ferrada, E. L. Droguett, V. Meruane, and M. Modarres, "Deep learning enabled fault diagnosis using time-frequency image analysis of rolling element bearings," Shock and Vibration, vol. 2017, 2017.

[17] S. Arif, M. J. Khan, N. Naseer, K.-S. Hong, H. Sajid, and Y. Ayaz, "Vector Phase Analysis Approach for Sleep Stage Classification: A Functional Near-Infrared Spectroscopy-Based Passive Brain–

Computer Interface," Frontiers in Human Neuroscience, vol. 15, p. 658444, 2021.

[18] T. Akhtar et al., "Effective Voting Ensemble of Homogenous Ensembling with Multiple Attribute-Selection Approaches for Improved Identification of Thyroid Disorder," Electronics, vol. 10, no. 23, p. 3026, 2021.

[19] T. Akhtar et al., "Ensemble-based Effective Diagnosis of Thyroid Disorder with Various Feature Selection Techniques," in 2nd International Conference of Smart Systems and Emerging Technologies (SMARTTECH), 2022, pp. 14–19: IEEE.

[20] I. Ali, Z. Mushtaq, S. Arif, A.-D. Algarni, N.-F. Soliman, and W. El-Shafai, "Hyperspectral Images-Based Crop Classification Scheme for Agricultural Remote Sensing," Computer Systems Science and Engineering, vol. 46, no. 1, pp. 303–319, 2023.

[21] S. Arif, M. Arif, S. Munawar, Y. Ayaz, M. J. Khan, and N. Naseer, "EEG Spectral Comparison Between Occipital and Prefrontal Cortices for Early Detection of Driver Drowsiness," in International Conference on Artificial Intelligence and Mechatronics Systems (AIMS), 2021, pp. 1–6: IEEE.

[22] J. Wang, Z. Mo, H. Zhang, and Q. Miao, "A deep learning method for bearing fault diagnosis based on time-frequency image," IEEE Access, vol. 7, pp. 42373–42383, 2019.

[23] Z. Lin, H. Ye, B. Zhan, and X. Huang, "An efficient network for surface defect detection," Applied Sciences, vol. 10, no. 17, p. 6085, 2020.